JOURNAL OF MATERIALS SCIENCE 25 (1990) 5063–5069

Solute partitioning on solidification of nickel-base ternary alloys

A. KAGAWA, M. HIRATA, Y. SAKAMOTO
Department of Materials Science and Engineering, Nagasaki University, Nagasaki 852, Japan

The coefficients for equilibrium partition of solute elements between solid and liquid were determined in nickel-base ternary alloys rapidly quenched from a coexisting solid–liquid state. A satisfactory accordance was observed between experimentally and theoretically determined partition coefficients, and factors influencing the ternary partition coefficients were clarified by a thermodynamic procedure. The availability of thermodynamic evaluation of the equilibrium partition coefficient was elucidated for application to nickel-base multicomponent alloys.

1. Introduction

In recent developments in super alloys, the design of materials plays an important part in fulfilling many requirements of appropriate properties for special applications. In processing super alloys, solute partitioning may give rise to inhomogeneous alloy composition which results in a local lack of expected properties and causes a lower level of restrictions for their applications. Hitherto, microsegregation of alloying elements, its effect on microstructure, and the effect of heat-treatment have been investigated [1–5] and equilibrium partition coefficients of solute elements have been determined in several nickel-base alloys [1, 2, 5]. The information is, however, limited to specific alloys and it should be pointed out that a fundamental understanding of solute partitioning is indispensable for the design of super alloys.

Microsegregation, which is closely related to partitioning of solute elements in the process of solidification, is an inherent phenomenon in most alloys and brings about detrimental problems in super alloys, such as inhomogeneous solute distribution [1, 3], formation of non-equilibrium phases and low melting-point eutectics [2], and local fluctuation of volume fraction of precipitates [4], which cause degradation in mechanical properties and oxidation and sulphidation resistances at high temperatures. Heat-treatment is not necessarily capable of diminishing dendritic segregation [4], and hence the selection of alloy chemistry to reduce dendritic segregation is of importance in the consideration of balancing other desired structures and properties. The key parameter characterizing partition behaviour of a solute element is its equilibrium partition coefficient which may be deduced from thermodynamic calculations provided thermochemical data are available.

In the present work, the coefficients of equilibrium partition of solute elements between solid and liquid were evaluated both experimentally and theoretically for nickel-base ternary alloys and the extension of the computation of partition coefficient to nickel base multicomponent alloys were investigated to elucidate its availability.

2. Experimental details

Nickel–silicon-base ternary alloys containing aluminium, cobalt, iron, chromium, molybdenum and tungsten were prepared by melting pure metals in an arc furnace. The purities of the metals were: > 99.2% Ni (Co < 0.03%), 99.999% Si, 99.99% Al, 99.5% Co, 99.99% Cr, 99.9% Fe, > 99% Mo, and > 99% W. After the inside of arc furnace was evacuated to less than 10^{-4} Pa and argon gas was introduced into it, pure titanium was melted as a getter of oxygen and, subsequently, about 20 g of the above mentioned metals were melted on a copper hearth cooled with water. The chemical compositions of the alloys are given in Table I.

For measurement of the equilibrium partition coefficients for solute elements between solid and liquid, about 10 g alloy was melted at 1753 K which was higher by about 100 K than the liquidus temperature predetermined by thermal analysis, and was cooled to a given temperature within the solidification temperature range. To attain equilibrium concentrations of solute elements in solid and liquid, the alloy was held at the temperature for 1 h, followed by quenching on a copper chill in a rapid cooling apparatus [6]. The liquidus and holding temperatures for the alloys are listed in Table II. The nickel–5 wt % silicon alloys has a solidification temperature range of about 100 K [7], thus the holding temperatures were taken to be about 10 K lower than the liquidus temperatures so that the fraction of solid would be about 0.1. This fraction of solid ensures the fluidity of a coexisting solid–liquid alloy on quenching and a small deviation from the equilibrium solute concentration in the centre of the dendrites leading to a shortened equilibrium period.

The surface of a quenched specimen in contact with the copper chill was polished and etched in a nitric acid–hydrochloric acid solution. The areas in both solid and liquid before quenching where the concentrations of solute elements were to be measured by an electron microprobe analyser were marked with Vickers microhardness indentations and then the surface was repolished to remove etch features ready to be subjected to electron microprobe analysis.

0022-2461/90 $03.00 + .12

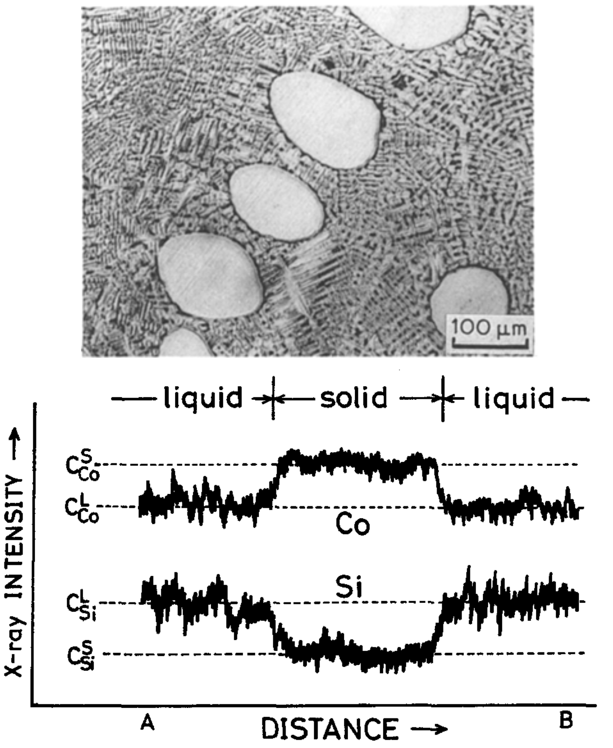

Figure 1 Microstructure and the distribution profiles of silicon and cobalt in the Ni–Si–Co quenched specimen.

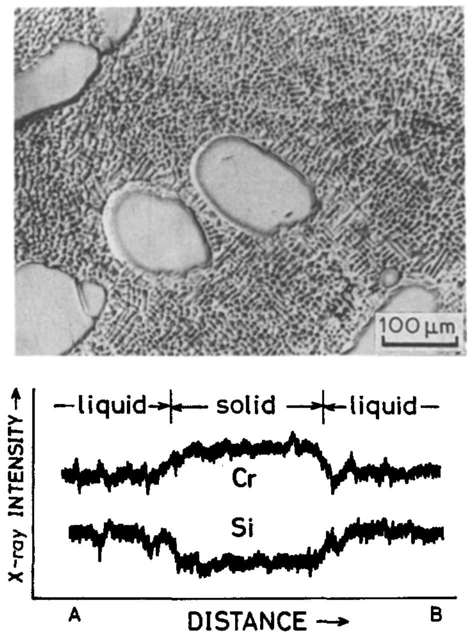

Figure 2 Microstructure and the distribution profiles of silicon and chromium in the Ni–Si–Cr quenched specimen.

3. Results

The microstructures and solute distribution profiles are shown in Figs 1 to 4, for quenched specimens of Ni–Si–Co, Ni–Si–Cr, Ni–Si–Mo and Ni–Si–W alloys, respectively. The shape of the primary solids in the sections examined are spherical, elliptical, or cylindrical and they are about 100 μm wide. The line-scanning profiles of solute concentrations in the solid region are relatively flat, except in the vicinity of solid–liquid interfaces.

The equilibrium partition coefficients of solute elements in nickel–silicon-base ternary alloys were determined as a ratio of the solute concentration in the solid region away from the interfaces to that in the liquid region before quenching, and are shown in Fig. 5, where the equilibrium partition coefficients in the nickel-base binary systems evaluated thermodynamically (Appendix 2) are given by the solid lines for silicon and the broken lines for the other elements for comparison. The binary partition coefficients can easily be estimated from the available phase diagrams. However, these partition coefficients might be erroneous and thus the thermodynamically evaluated ones are adopted.

Cobalt and iron have equilibrium partition coefficients of almost unity in the nickel-base binary systems, while in the nickel–silicon-base ternary alloys, these elements were captured in the primary solids during solidification, e.g. an example for cobalt is shown in Fig. 1. This means that the equilibrium partition coefficients of these elements are larger than unity. This is the case of "newly introduced segregation" produced by an addition of silicon. As can be seen in Fig. 2, the chromium concentration in the solid region is higher than that in the liquid region before quenching and chromium is enriched in the primary solid during solidification. Thus the equilibrium partition coefficient of chromium is larger than unity. In the nickel–chromium binary system, chromium has an equilibrium partition coefficient less than unity, and hence, the addition of 5% silicon has the effect of "inverting" the segregation of chromium in the binary alloy. A similar effect was observed in the Ni–Si–Al alloy. In the Ni–Si–Mo alloy, the segregation tendency of molybdenum was somewhat reduced by an addition of silicon ("reduced segregation"). In the Ni–Si–W alloy, the "enhanced segregation" of tungsten by silicon was observed where the equilibrium partition coefficients of tungsten in the ternary alloy and in the nickel–tungsten binary system are larger than unity and the former is larger than the latter. In all the ternary alloys, the equilibrium partition coefficient of silicon remains less than unity, and

TABLE I Chemical compositions of the alloys used

Alloy	Chemical composition (wt %)							
	Ni	Si	Al	Co	Cr	Fe	Mo	W
Ni–5Si	Balance	4.79	–	–	–	–	–	–
Ni–5Si–Al	Balance	5.10	2.84	–	–	–	–	–
Ni–5Si–Co	Balance	5.12	–	3.28	–	–	–	–
Ni–5Si–Cr	Balance	4.91	–	–	3.20	–	–	–
Ni–5Si–Fe	Balance	5.09	–	–	–	3.06	–	–
Ni–5Si–Mo	Balance	4.97	–	–	–	–	3.22	–
Ni–5Si–W	Balance	5.30	–	–	–	–	–	3.34

TABLE II Liquidus and holding temperatures of the specimens

Specimen	Liquidus temperature (K)	Holding temperature (K)
Ni–5Si	1639	1630
Ni–5Si–3Al	1632	1624
Ni–5Si–3Co	1620	1611
Ni–5Si–3Cr	1618	1609
Ni–5Si–3Fe	1620	1612
Ni–5Si–3Mo	1619	1612
Ni–5Si–3W	1632	1624

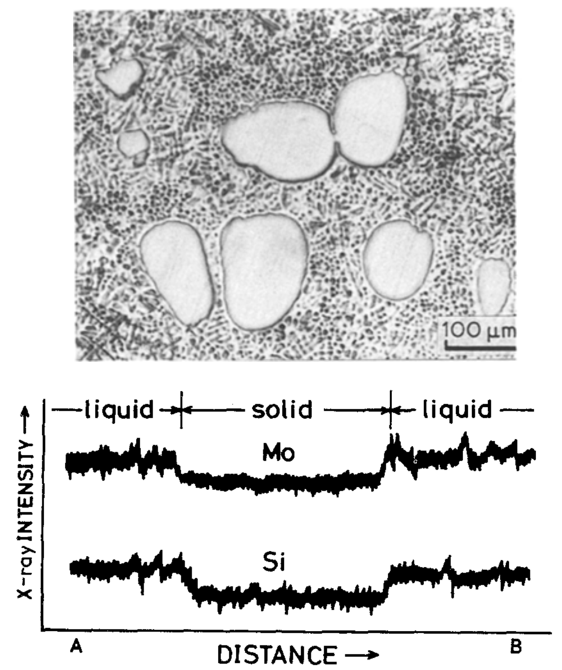

Figure 3 Microstructure and the distribution profiles of silicon and molybdenum in the Ni–Si–Mo quenched specimen.

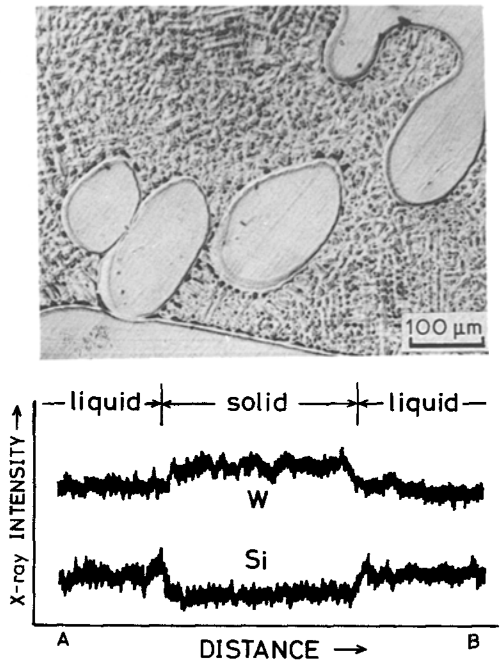

Figure 4 Microstructure and the distribution profiles of silicon and tungsten in the Ni–Si–W quenched specimen.

there is little significant influence of the interaction between a third element and silicon.

4. Discussion

4.1. Effects of holding period and back diffusion on the accuracy of the observed partition coefficient

In the present work, a coexisting solid–liquid state was frozen by a rapid quenching to determine equilibrium partition coefficients of solute elements. The accuracy of the obtained partition coefficients depends not only on the accuracy of the electron microprobe analysis but also on the holding period in a coexisting solid–liquid state and the subsequent cooling conditions. In the following paragraphs, the solute diffusion in the primary solid during holding and the back-diffusion distances during quenching were evaluated using one-dimensional diffusion models. The computation methods are given in Appendix 1.

The solute concentration in a solid crystallized at the liquidus temperature is given by $C_S = k_0 C_0$, where k_0 is the equilibrium partition coefficient of an element X and C_0 is the concentration of the element X in an alloy. As the time elapsed for the crystallization of a primary solid of 0.1 weight fraction during cooling from the liquidus temperature to the holding temperature was a few minutes, diffusion of solute elements in the solid can be negligible in such a short time interval, even for silicon which has the largest diffusion coefficient in this experiment. Therefore, the solute distribution in the solid at the beginning of holding can be given by the Sheil equation [8]

$$C_S = k_0 C_0 (1 - f_S)^{(k_0 - 1)} \qquad (1)$$

where f_S is the fraction solidified. The solute-concentrations in the solid and liquid at the solid–liquid interface are given by the following equations

$$C_S^* = k_0 C_0 (0.9)^{(k_0 - 1)} \qquad (2)$$

$$C_L^* = C_S^* / k_0 \qquad (3)$$

If an effective partition coefficient is defined as $k_e = C_S / C_L^*$, the maximum deviation of the effective

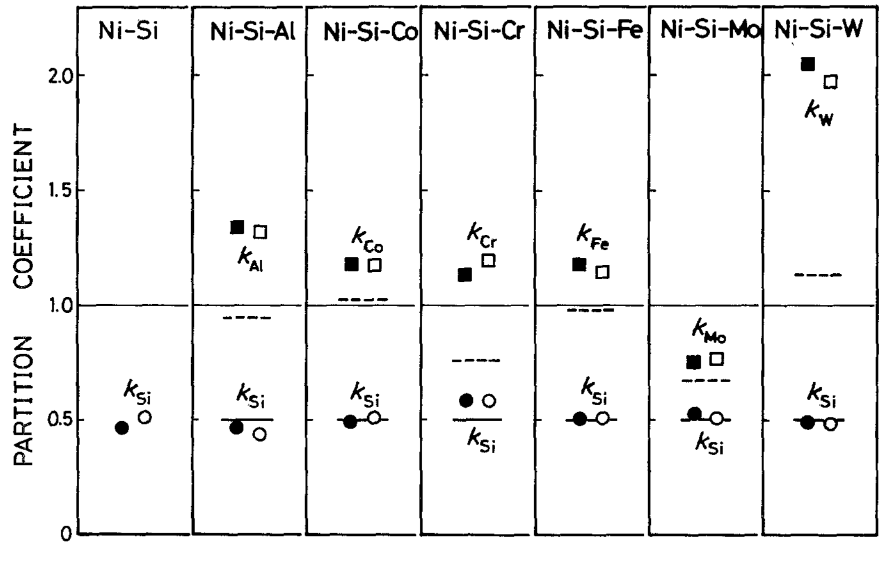

Figure 5 Equilibrium partition coefficients of solute elements in Ni–Si–X (X = Al, Co, Cr, Fe, Mo and W) ternary alloys; (●, ■) experimental, (○, □) calculated, (——) Ni–Si binary alloy, (- - -) Ni–X binary alloys.

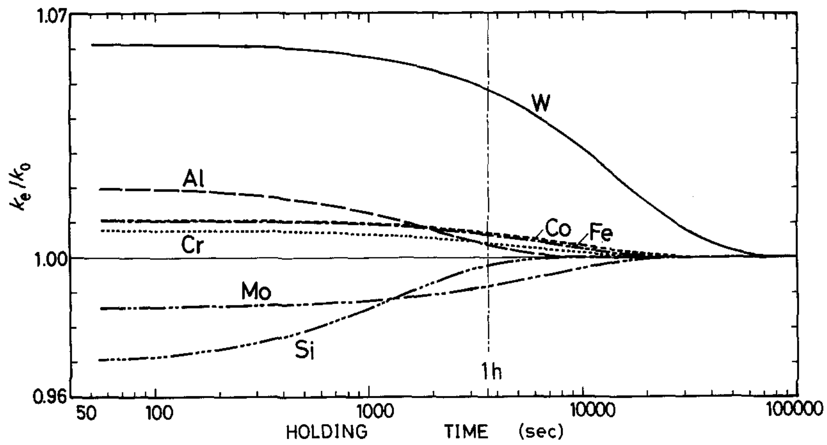

Figure 6 Variations in a ratio of the partition coefficients k_e/k_0 for solute elements in Ni-Si-base ternary alloys with holding period.

partition coefficient from the equilibrium one can be evaluated by a ratio of k_e/k_0 ($= (0.9)^{(1-k_0)}$). The ratio for silicon ($k_0 = 0.5$) is 0.95 and that for tungsten ($k_0 = 2$) is 1.11, leading to errors of about 5% and 11% in the effective partition coefficients.

In the electron microprobe analysis, the solute concentration in the solid as well as in the liquid is taken as an average, except in the vicinity of the solid–liquid interface, and if we take the average solute concentration in the solid, $\bar{C}_S$ ($= \int_0^{0.1} C_S \, df_S/f_S$) instead of C_S, the errors are reduced to less than 3% for silicon and 6% for tungsten. This means that in the method employed in the present work, the maximum error in a measured partition coefficient due to inhomogeneous solute distribution in the solid is at most 6% for severe segregating elements such as tungsten. It is, therefore, noted that holding in a coexisting solid–liquid state has two objectives: (1) further homogenization of solute distribution which reduces the error due to inhomogeneous solute distribution, and (2) coarsening of the primary solid to a proper size for distinction from other primary solids formed during quenching and for the subsequent electron microprobe analysis. The ratios of k_e/k_0 ($k_e = \bar{C}_S/C_L^*$) for solute elements were calculated by the explicit method where the size of the primary solid was taken to be 100 μm. Because this size should be a resultant of coarsening during holding, it is thought that the calculation may give a longer holding period for homogenization. In Fig. 6, the values of k_e/k_0 are plotted as a function of holding period. The holding time of 1 h gives a maximum error less than 1% due to inhomogeneous distribution of solute elements in the measured partition coefficients except tungsten. A holding period of about 7.5 h is required to ensure an error within 1% for tungsten. The standard deviations of the measured solute concentration in more than ten solid particles in the electron microprobe analysis was less than 5% and thus the total error in an observed partition coefficient was estimated by $\Delta p_{\mathrm{total}} = \Delta p_{\mathrm{inhom}} + \Delta p_{\mathrm{meas}}$. The expected error in the partition coefficient for tungsten amounts to about 10%. On the other hand, the resulting errors in the observed partition coefficients shown in Fig. 5 were 6% for tungsten and less than 5% for others. The smaller error in the observed partition coefficient for tungsten than that expected, possibly arises from the effect of coarsening, the approximation with one-dimensional diffusion model, and/or the electron microprobe analysis on the off-centred sections of solid particles in the sample.

4.2. Effect of back-diffusion during quenching on solute distribution

The solute concentration in the liquid at the solid–liquid interface increases during quenching for an element having a partition coefficient smaller than unity, and hence the concentration in the solid in equilibrium with that in the liquid also increases, causing the back diffusion of the element from the interface into the solid. Because silicon as an alloying element in the present work has the largest diffusivity, its back diffusion distance was evaluated by the explicit method described in Appendix 1. The cooling rate from a coexisting solid–liquid state was given as 1000, 600, 300, or 150 K sec^{-1} which would correspond to the case of oil-quenching [9]. The diffusion

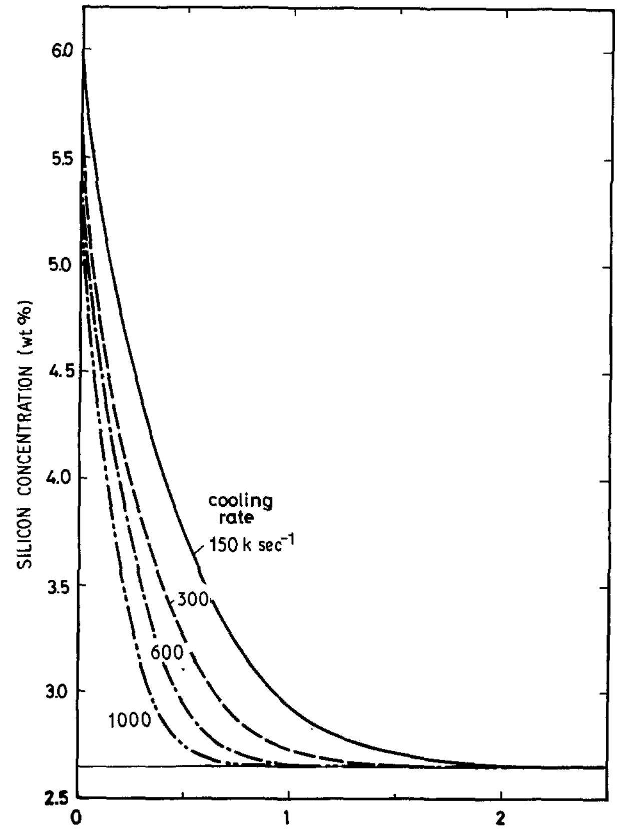

Figure 7 Back-diffusion distances of silicon during quenching of the Ni–5 wt % Si alloy for various cooling rates.

simulation was performed until the temperature decreased by 300 K below the solidus, which was determined as a temperature where the fraction of solid became unity in the calculation. The result is shown in Fig. 7. The back-diffusion distance for silicon was at most 2 μm for the slowest cooling rate, and other elements with smaller diffusion coefficients than that of silicon should be less. It is, therefore, ensured that there is no effect of back diffusion on the observed partition coefficients if the solute concentrations, exclusive of those in the vicinity of the solid–liquid interface, are adopted in determining the partition coefficients.

4.3. Thermodynamic evaluation of the partition coefficient

To elucidate the availability of the thermodynamic evaluation the equilibrium partition coefficients of solute elements in nickel-base ternary alloys were computed using the thermochemical data given in the literature [6, 10–14]. The details of the calculation are described in Appendix 2. In Fig. 5, the calculated partition coefficients of solute elements are shown by open circles and squares. A satisfactory agreement is seen between the calculated partition coefficients and the experimental ones given by solid circles and squares, indicating that the thermodynamic evaluation is useful in determining the ternary partition coefficients and suggesting that it can be applied to the multicomponent systems. The experimental values of equilibrium partition coefficients of solute elements were given by Sellamuthu and Giamei [1] for MAR-M200 which was taken to be a hexanary alloy Ni–Co–Cr–W–Al–Ti, although it contains an additional four minor elements (carbon, niobium, zirconium and boron). The equilibrium partition coefficients of five solute elements were computed by the procedure extended to the hexanary system. The calculated values are listed in Table III, together with the experimental ones given by Sellamuthu and Giamei. In determining the equilibrium partition coefficients, they employed a plane front solidification technique where the effect of diffusion of solute elements on their distribution profiles may be negligible and the possible error in their partition coefficients can be ascribed to that in the electron microprobe analysis. In comparison with the experimentally determined partition coefficients, the calculated values exclusive of that for chromium are in fair agreement with the experimental ones within a difference of 5%. For chromium, the discrepancy is about 16% which may give a maximum superposed error resulting from the accuracy of thermodynamic data and the procedures of both the experiment and analysis. The result represented in Table III reveals the availability of thermodynamic evaluation for the equilibrium partition coefficients of solute elements in nickel-base multicomponent systems.

TABLE III Equilibrium partition coefficients of solute elements in the nickel-base multicomponent alloy (Mar-M200)

Element X	(wt %)	Partition coefficient (k)		($\Delta k/k$) × 100† (%)
		Calculated	Experimental*	
Co	10.5	1.09	–	–
Cr	9.4	0.78	0.93	−16.1
W	11.8	1.37	1.31	4.6
Al	4.5	0.82	0.86	4.7
Ti	2.1	0.57	0.60	5.0

*[1].

†$(\Delta k/k) = (k_{\text{cal}} - k_{\text{exp}})/k_{\text{exp}}$.

4.4. Factors influencing ternary partition coefficient

In an Ni–X–Y ternary system, the equilibrium partition coefficient of element X is represented by the sum of the following three terms. (see Appendix 2)

$$\ln k_{\mathrm{X}} = F1 + F2 + F3 \tag{4}$$

$$F1 = \ln(\dot{\gamma}_{\mathrm{X}}^{\mathrm{L}}/\dot{\gamma}_{\mathrm{X}}^{\mathrm{S}}) + (\dot{\mu}_{\mathrm{X}}^{\mathrm{L}} - \dot{\mu}_{\mathrm{X}}^{\mathrm{S}})/RT \tag{5}$$

$$F2 = (\varepsilon_{\mathrm{X}}^{\mathrm{XL}} - \varepsilon_{\mathrm{X}}^{\mathrm{XS}} k_{\mathrm{X}}) N_{\mathrm{X}}^{\mathrm{L}} \tag{6}$$

$$F3 = (\varepsilon_{\mathrm{X}}^{\mathrm{YL}} - \varepsilon_{\mathrm{X}}^{\mathrm{YS}} k_{\mathrm{Y}}) N_{\mathrm{Y}}^{\mathrm{L}} \tag{7}$$

The term $F1$ is characterized by the thermochemical nature of the element X, $F2$ is its concentration dependence term, and $F3$ is an interaction term between the elements X and Y. Figs 8 and 9 show the contribution of these factors to the partition coefficient of the element X in Ni–Si–X (X = Al, Co, Cr, Fe, Mo and W) alloys, where a lowering of temperature in the abscissa means a decrease in the liquidus temperature with increasing silicon content. It is known from Figs 8a and c that the "inversion" in the segregation tendency of aluminium and chromium in the Ni–Si–Al and Ni–Si–Cr alloys is attributable to factor $F3$, i.e. the interaction between aluminium or chromium and silicon. In Fig. 8b, it is noted that the "newly introduced segregation" of cobalt in the Ni–Si–Co alloy is not caused by the interaction between cobalt and silicon but by a reduction of solidification temperature with

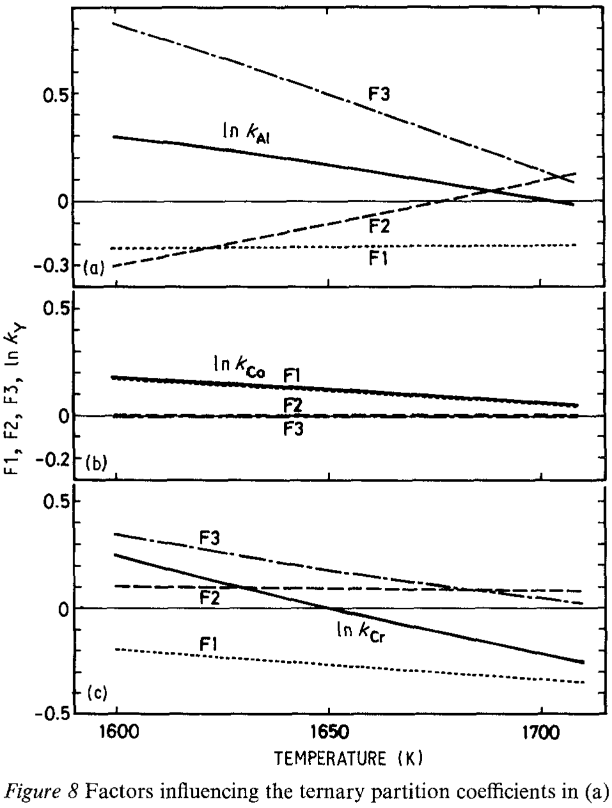

Figure 8 Factors influencing the ternary partition coefficients in (a) Ni–Si–Al, (b) Ni–Si–Co and (c) Ni–Si–Cr alloys.

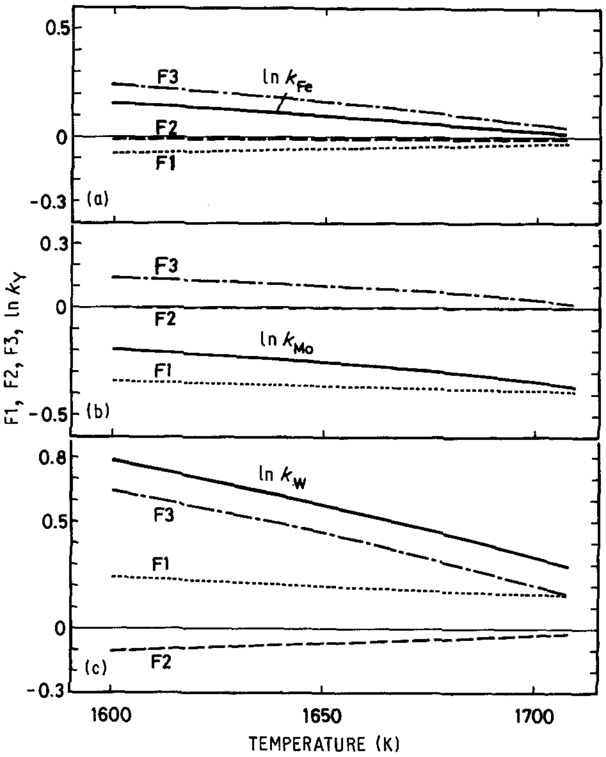

Figure 9 Factors influencing the ternary partition coefficients in (a) Ni–Si–Fe, (b) Ni–Si–Mo and (c) Ni–Si–W alloys.

increasing silicon content, through factor $F1$, while in the Ni–Si–Fe alloy shown in Fig. 9a, the contribution of factor $F3$ is the reason for an increased partition coefficient of iron. In Fig. 9b, the equilibrium partition coefficient of molybdenum increases with increasing silicon content in the Ni–Si–Mo alloy and the "reduced segregation" tendency of molybdenum is ascribed to factor $F3$, i.e. a repulsive interaction between molybdenum and silicon. In the case of the Ni–Si–W alloy shown in Fig. 9c, factors $F2$ and $F3$ act in opposite ways as is the case in the Ni–Si–Al and Ni–Si–Cr alloys and the latter is predominant in determining the partition coefficient at a lower temperature, resulting in the "enhanced" segregation of tungsten. The results given in these figures demonstrate that equilibrium partition coefficients of solute elements in a multicomponent alloy would change by not only the interaction between solute elements but also a variation of solidification temperature with additives. For the latter reason, alloying elements such as carbon, silicon and titanium are harmful when the added amounts of these elements increase.

5. Conclusion

The equilibrium partition coefficients of solute elements between solid and liquid were determined for nickel-silicon-X (X = Al, Co, Cr, Fe, Mo, W) ternary alloys rapidly quenched from a coexisting solid-liquid state. The accuracy of the measured partition coefficients depends on the holding period in a coexisting solid-liquid state and the procedure of analysing solute concentrations as well as inherent errors in electron microprobe analysis. There is a precise size of primary solid for homogenization of solute concentrations in it, for maintaining fluidity, and for the subsequent electron microprobe analysis. Selecting the holding temperature to obtain a weight fraction of about 0.1 and the holding period, such an adequate solid size of the order of 100 μm was obtained. Back-diffusion distances of the diffusion species during rapid quenching were less than 2 μm, which gave an insignificant effect on solute distribution in primary solid. The total error in the obtained equilibrium partition coefficients was at most 6%.

The equilibrium partition coefficients calculated using the available thermochemical data were in good accordance with the experimental ones, establishing the advantages of the thermodynamical evaluation of equilibrium partition coefficients of solute elements in nickel-base ternary and multicomponent alloys. From an analysis of ternary partition coefficients, it was demonstrated that the factors influencing the partition coefficients included the effect of an alloying element on solidification temperature as well as that of solute interaction between the species.

Appendix 1

Solute distribution in a primary solid after cooling from the liquidus temperature to a holding temperature can be represented by the Scheil equation (no solid diffusion and complete mixing in the liquid)

$$C_S = k_0 C_0 (1 - f_S)^{(k_0 - 1)} \tag{A1}$$

where C_S and C_0 are solute concentrations in the solid

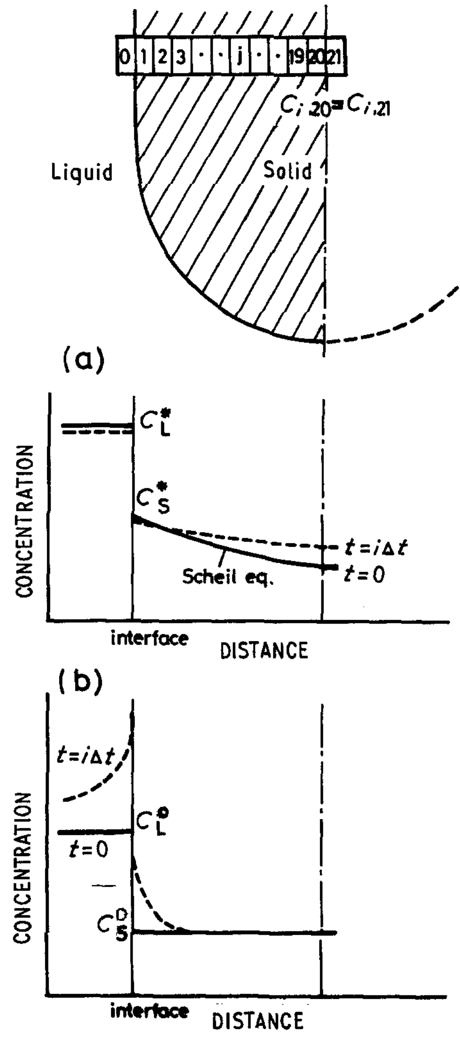

Figure A1 Simulation models for (a) diffusion during holding an alloy in a coexisting solid–liquid state, and (b) evaluation of a back-diffusion distance during quenching.

and an alloy, respectively, k_0 is the equilibrium partition coefficient of a solute element, and f_S is the fraction solidified. The diffusion model for the computation of solute distribution profiles using the explicit method is illustrated in Fig. A1a. The difference equation to calculate a solute concentration in a solid based on Fick's law is given by

$$\begin{aligned} C_{i,j} &= C_{i-1,j} \\ &\quad + D\Delta t(C_{i-1,j-1} - 2C_{i-1,j} + C_{i-1,j+1})/(\Delta x)^2 \end{aligned} \tag{A2}$$

where i, j are time (t) and distance (x) steps, respectively, and D is the diffusion coefficient of a solute element in a solid.

Initial and boundary conditions are given by Equations A3 and A5

$$C_{0,j} = k_0 C_0 (1 - f_S)^{(k_0 - 1)} \tag{A3}$$

$$f_S = 0.1(n + 1 - j) \tag{A4}$$

$$\begin{aligned} C_{i,0} &= C_S^* \\ &= k_0 C_L^* \end{aligned} \tag{A5}$$

$$C_L^* = \left(1 - \sum_j C_{i,j}\Delta x\right) \Big/ (1 - f_S) \tag{A6}$$

where n is the number of divided elements, C_S^* and C_L^* are solute concentrations in the solid and liquid at the solid–liquid interface, respectively. The solute distribution profile at the beginning of holding is affected by the shape of a primary solid. Assuming its shape is cylindrical, the relationship between distance x and fraction of solid f_S in Equations A3 and A6 is given by

$$f_S = 0.1(j\Delta x)^2 \tag{A7}$$

Although the solute diffusion in a cylindrical solid during holding is two-dimensional, it is approximated by one-dimensional diffusion for simplification and this treatment gives a slightly longer holding period for homogenization.

The model for evaluating a back-diffusion distance is shown in Fig. A1b. A similar explicit method is applied where the initial and boundary conditions are given by Equations A8 and A9

$$C_{0,j} = C_S^0 \tag{A8}$$

$$C_{i,0} = kC_L(T) \tag{A9}$$

$$T = T_h - V\Delta t \tag{A10}$$

where C_S^0 is an equilibrium solute concentration in the primary solid before quenching, $C_L(T)$ is the solute concentration on the liquidus as a function of temperature T, T_h is a holding temperature, and V is a cooling rate.

Appendix 2

In an Ni–X–Y ternary system, the equilibrium conditions for the elements X and Y are given by the following equations

$$\begin{aligned} \ln k_X &= \ln(\dot{\gamma}_X^L/\dot{\gamma}_X^S) + (\dot{\mu}_X^L - \dot{\mu}_X^S)/RT \\ &\quad + (\varepsilon_X^{XL} - \varepsilon_X^{XS}k_X)N_X^L + (\varepsilon_X^{YL} - \varepsilon_X^{YS}k_Y)N_Y^L \end{aligned} \tag{A11}$$

$$\begin{aligned} \ln k_Y &= \ln(\dot{\gamma}_Y^L/\dot{\gamma}_Y^S) + (\dot{\mu}_Y^L - \dot{\mu}_Y^S)/RT \\ &\quad + (\varepsilon_Y^{YL} - \varepsilon_Y^{YS}k_Y)N_Y^L + (\varepsilon_Y^{XL} - \varepsilon_Y^{XS}k_X)N_X^L \end{aligned} \tag{A12}$$

where k_i is the coefficient for equilibrium partition of the element i between solid (S) and liquid (L), $\dot{\gamma}_i^v$ and $\dot{\mu}_i^v$ are the activity coefficient of the element i at infinite dilution and the chemical potential of the pure element i in v phase (v = L or S) respectively, ε_i^{jv} is an interaction coefficient between the elements i and j in v phase, N_i^L is a mole fraction of the element i in liquid, R is the gas constant, and T is the temperature where solid and liquid phases are in equilibrium. The values of $\dot{\gamma}_i^L$, $\dot{\gamma}_i^S$, $(\dot{\mu}_i^L - \dot{\mu}_i^S)$, ε_i^{jL} and ε_i^{jS} in the equations are given in the literature [6, 10–14]. If we take the concentrations of elements X and Y in an alloy as N_X^L and N_Y^L, these equations involve two unknown parameters of k_X and k_Y. The equilibrium partition coefficients of elements X and Y at the liquidus temperature were determined by solving simultaneous equations of Equations A11 and A12. In a nickel-base hexanary system, the equilibrium partition coefficients of solute elements were similarly obtained by solving five simultaneous equations for five solute elements.

References

1. R. SELLAMUTHU and A. F. GIAMEI, *Met. Trans.* **17A** (1986) 419.
2. M. A. TAHA and W. KURZ, *Z. Metallkde* **72** (1981) 546.
3. I. L. SVETLOV, N. V. PETRUSHIN, V. A. FEDOROV and N. P. ABALAKIN, *Phys. Met. Metall.* **57** (1984) 111.
4. K. M. DELARGY and G. D. W. SMITH, *Met. Trans.* **14A** (1983) 1771.
5. M. SITTNER, *J. Crystal Growth* **65** (1983) 299.
6. A. KAGAWA, S. MORIYAMA and T. OKAMOTO, *J. Mater. Sci.* **17** (1982) 135.
7. T. B. MASSALSKY, "Binary Alloy Phase Diagrams" (ASM, New York, 1986) p. 1756.
8. E. SCHEIL, *Z. Metallkde* **34** (1942) 70.
9. T. OKAMOTO, Z. MORITA, A. KAGAWA and T. TANAKA, *Trans. Iron Steel Inst. Jpn* **23** (1983) 266.
10. L. KAUFMAN and H. NESSOR, *Z. Metallkde* **64** (1973) 249.
11. *Idem, CALPHAD* **2** (1978) 55.
12. *Idem, ibid.* **2** (1978) 81.
13. *Idem, ibid.* **2** (1978) 325.
14. *Idem, ibid.* **3** (1979) 45.

Received 27 April
and accepted 8 September 1988